FORESTRY IDEAS, 2023, vol. 29, No 2 (66): 300–313

Using the regression model to estimate the infiltration rate from soil properties after shifting cultivation in Vietnam

Tran Xuan Minh*, Nguyen Dinh Vinh, Ta Thi Binh, Hoang Thi Mai, and Nguyen Thi Huong Giang

Institute of Agriculture and Natural Resources, Vinh University, Nghean 43000, Vietnam.
*E-mail: minhtx@vinhuni.edu.vn

Received: 23 February 2023 / Accepted: 13 November 2023 / Available online: 20 November 2023

Abstract

The aim of the study was: (i) to measure the different soil properties and infiltration rate; (ii) to determine the optimum soil infiltration rate model based on soil properties (soil porosity, bulk density, soil moisture, organic matter, clay, silt and sand) after shifting cultivation in Vietnam. Infiltration rates were measured using a double-ring infiltrometer at 36 sampling points, and the measurements were taken from February to June 2020. Location of each infiltration stations were marked using GPS device. The results showed that the infiltration rate in vegetation recovering (grassland, shrubland and small regenerating trees) after shifting cultivation varied from 2.41 to 3.23 mm·min^{-1}, with an average measured infiltration rate of 2.87 ±0.22 mm·min^{-1}. The soil porosity, organic matter content and sand have a positive correlation with infiltration rate, whereas bulk density, soil moisture, clay, silt have a negative one. The analysis performed for five models considering the combination of soil properties and subjected to regression analysis. Result showed that in order to predict soil infiltration rate based on few properties of soil with four independent variables, multi-linear regression model *IR* = 1.745 + 0.026 (*SP*) + 0.016 (*OM*) - 0.026 (*SM*) + 0.003 (sand) with the coefficient of determination R^2 = 0.856, Bayesian Information Criterion (*BIC*) = -55.77 and posterior probability = 15.5 % is the best model for the estimation of infiltration rate and recommended for the research area.

Key words: bulk density, multi-linear regression, organic matter, soil moisture, soil porosity.

Introduction

Soil infiltration plays an important role in water storage for crops due to its direct effect on rainfall and crop yields and volume, transport routes and agricultural drainage quality (Huang et al. 2017). In arid and semi-arid regions, where precipitation is lower than evaporation, managing to get enough water is essential to sustaining plant life (Tang et al. 2018). In addition, soil infiltration is related to the risk of water erosion, as the main impact of soil erosion is runoff and residual water content on the soil surface after infiltration (Moazeni-Noghondar et al. 2021).

The initial infiltration rate, average infiltration rate, stable infiltration rate, or infiltration rates of several different stages were used to evaluate the stage characteristics of the infiltration process (Li et al. 2013, Zhao et al. 2013, Tang et al. 2018, Zhu et al. 2020). Neris et al. (2012) used the steady-state infiltration rate to study the effect of vegetation types on soil-water infiltration. Reynolds and Reddy (2012) used the average infiltration rate to assess the soil infiltration capacity in reclaimed surface coal mines. However, soil infiltration processes cannot be well described by one or two types of infiltration rates because they contain different information.

Traditional studies indicated that soil infiltration was affected by soil texture and structure (Saputra et al. 2022). It is one of the primary factors affecting infiltration characteristics. However, subsequent studies showed that infiltration was not only affected by soil texture but also by soil properties (Tang et al. 2018, Karahan and Yalim 2022). Soil bulk unit weight has an inverse correlation with infiltration rate. Higher soil bulk density reduces soil porosity, leading to decreased infiltration characteristics. Initial moisture content is a critical parameter that affects water retention and transmission in soil. According to Pandey and Pandey (2018), the hydraulic conductivity of sandy soil decreases with depth. Hence, the initial moisture content is a key input variable for modelling soil infiltration characteristics. Characterizing infiltration at the field scale is challenging due to the need for multiple measurements (Khatri and Smith 2005). Estimating infiltration features is difficult because of significant spatiotemporal variability. To address these challenges, researchers globally (Mirzaee et al. 2014, Parhi 2014, Tuffour and Bonsu 2015) have suggested using infiltration models as an alternative to field-based measurements. Linear and non-linear regression are widely used approach (Rahmati 2017).

Shifting cultivation affects the hydrologic balance, creating unregulated stream flows and increasing the risk of soil erosion, floods and droughts (Schröder et al. 2023). The main cause of these problems is increased runoff due to low infiltration rate and a decrease in soil water retention (Morbidelli et al. 2018). Many studies have reported the changes in soil infiltration and soil properties after forest clearing for agricultural purposes (Sajjadi et al. 2016, Patle et al. 2018, Sun et al. 2018, Dionizio and Costa 2019, Karahan and Yalim 2022).

In view of above, an attempt was conducted to predict the soil infiltration rate of vegetation recovered after shifting cultivation using the Multiple Linear Regression Analysis with the following objectives: (i) to measure the different soil properties and infiltration rate of vegetation recovered after shifting cultivation; (ii) to determine the optimum soil infiltration rate model based on soil properties.

Materials and Methods

Study area

The study area is a mountainous district located in the southwest of Nghe An province, Vietnam (19°18’28” N and 104°28’36” E), and was performed from February to June 2020. Nghe An is directly affected by the tropical monsoon climate. The average temperature varies from 23–25 °C. The average rainfall is 1450 mm but unevenly distributed in space and time. The shifting cultivation area is 50,000 ha. As the vegetation in the area is mainly composed of grasslands and shrublands

growing on fallow swidden, these areas will be the focus of development and rehabilitation measures in the coming period. The aim of these efforts is to promote the forest protection function and provide sustainable land use practices.

Thirty-six study sites corresponding to the three different vegetation types after shifting cultivation (grassland, shrubland and small regenerating trees) were selected within the area described above (Fig. 1). As shown in Figure 1, twelve of the sites were grasslands that had formed after 1–3 years of fallow in shifting cultivation. Fifteen of the sites were shrublands where the number of regenerating trees was less than 500 trees·ha^{-1} and they had formed after 4–6 years of fallow. Nine of the sites were small regenerating trees; the number of regenerating trees with a height over 1 m was 1000 trees·ha^{-1} and they had formed after 7–9 years of fallow.

Soil sampling and analysis

Thirty-six surface soil samples were collected from the topsoil (0–20 cm soil layer) with a steel cutting ring (5 cm in diameter and 5 cm in depth) for further analysis of basic soil properties. The collected soil samples were placed in plastic-lined soil bags and transported to the laboratory. Moist soil samples were air-dried at room temperature and large roots were removed.

Soil bulk density (*BD*) was measured by a soil bulk sample with a 5 cm diameter and a 5 cm-high stainless steel cutting ring (three replicates). It was calculated by formulas (1):

$$BD = \frac{w_2 - w_1}{v}, \quad (1)$$

where: *BD* is bulk density, g·cm^{-3}; W_1 is the weight of core cutter, g; W_2 is the weight of core cutter and soil, g; *V* is the volume of core cutter, cm^3 (Patle et al. 2019).

A soil sample for estimating soil moisture (*SM*) was collected nearby before infiltration and *SM* was determined using the oven drying method, keeping soil samples at 150 °C for 24 h. The *SM* was calculated by formulas (2):

$$SM = \frac{M_0 - M_1}{M_0}, \quad (2)$$

where: *SM* is soil moisture content, %; M_0 is weight of soil, g; M_1 is weight of dried soil, g (Patle et al. 2019).

Soil porosity (*SP*) was calculated by formulas (3):

$$SP = \left(1 - \frac{BD}{RD}\right) \cdot 100, \quad (3)$$

where: *SP* is the total soil porosity, %; *BD* is the soil bulk density, g·cm^{-3}; *RD* is relative density, g·cm^{-3}.

Determination of particle size distribution of soil samples has been analysed by Pipette method (Gee and Bauder 1986). The particle size distribution was calculated by formulas (4–6):

$$\text{Clays} = \frac{(m_2 - m_B) \cdot 10^5}{V_p \cdot m \cdot K}, \quad (4)$$

$$\text{Silts} = \frac{(m_1 - m_2) \cdot 10^5}{V_p \cdot m \cdot K}, \quad (5)$$

$$\text{Sands} = \frac{100 \cdot m_3}{m \cdot K}, \quad (6)$$

where: *m* is mass of soil sample (air dried); m_1 is mass of first sample (clay + silt) after drying 105 °C; m_2 is mass of second sample (clay) after drying 105 °C; m_3 is mass of total sands after drying 105 °C; *K* is moisture correction coefficient = mass sample after drying at 105 °C·m^{-1}; V_p is volume of the sample; m_B is mass of blank (reagents without sample) after drying 105 °C.

The measurement of soil organic matter (*OM*) content was determined by oxidation with the potassium chromate method by formulas (7 and 8):

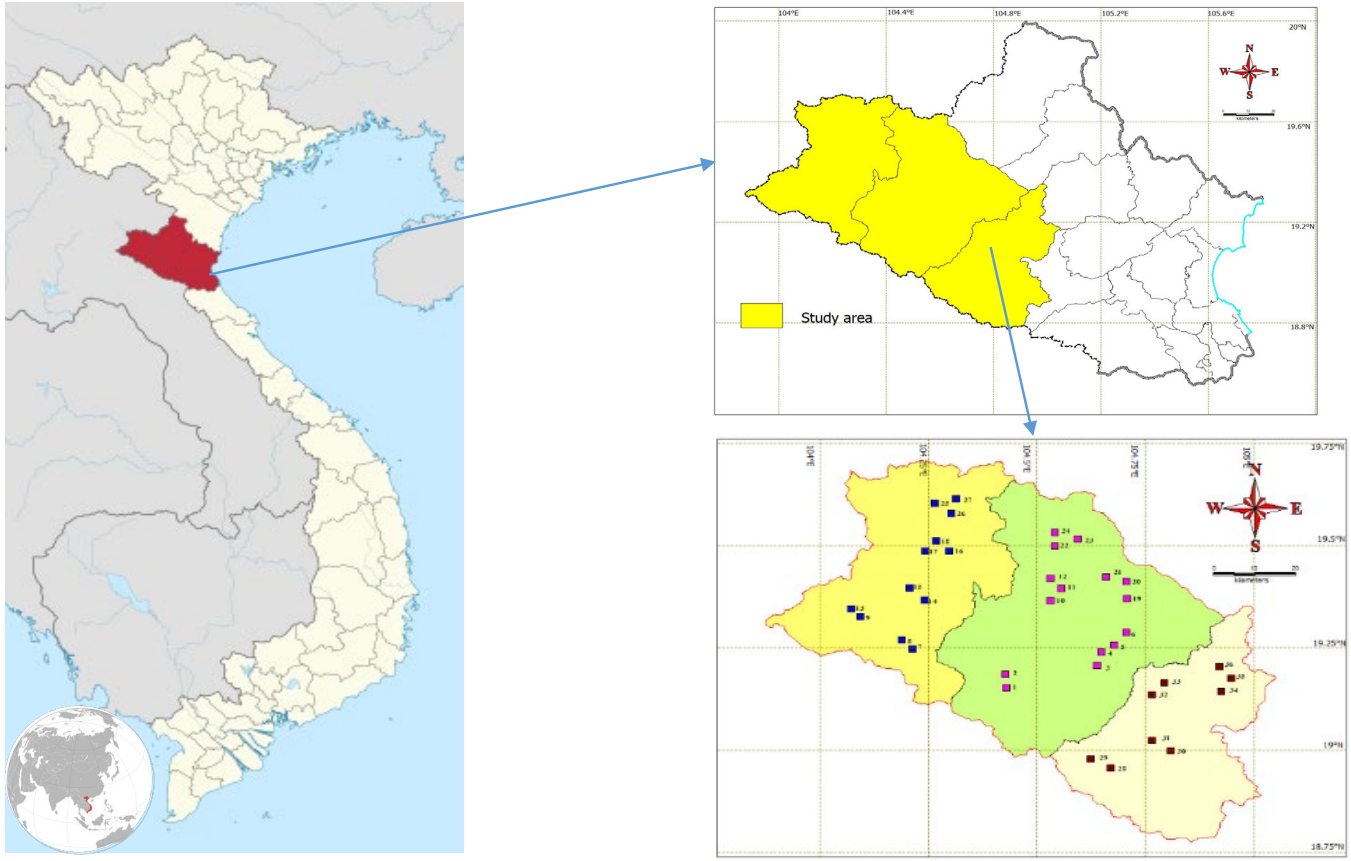

Fig. 1. Map of study area and experimental plots.

Note: Twelve of the dark blue boxes represented grassland sites that had developed after 1–3 years of fallow in shifting cultivation; fifteen of the pink boxes represented shrublands sites that had developed after 4–6 years of fallow in shifting cultivation; nine of the brown boxes represented shrublands sites that had developed after 7–9 years of fallow in shifting cultivation.

$$\text{Organic carbon (\%)} = 1.334 \cdot \frac{(V_b - V_s) \cdot 0.3 \cdot M}{W_t}, \quad (7)$$

$$\text{Organic matter (\%)} = 1.724 \cdot \text{organic carbon}, \quad (8)$$

where: V_b and V_s are the titration volume of blank sample and volume of soil sample respectively, mL; $0.3 \cdot M$ is the molarity of $(NH_4)_2SO_4$ and $FeSO_4 \cdot 6H_2O$ solution used in the titration; W_t is the soil sample weight, g (Farid et al. 2019).

Infiltration rate measurement

Infiltration rates were measured by using a double-ring infiltrometer on 36 sample plots. A constant head of water 3 cm deep was maintained in both the 20 cm diameter inner ring and the 30 cm diameter buffer (outer) ring. The average infiltration rate during the 0–110 min period is defined as the overall average infiltration rate (*IR*) (Wu et al. 2016). Calculating soil-water infiltration rate by formula (9):

$$IR = \frac{Q \cdot 10}{S \cdot T}, \quad (9)$$

where: *IR* is the water infiltration rate of soil, $mm \cdot min^{-1}$; *Q* is the amount of water absorbed, cm^3; *S* is ring cutter cross-section area, cm^2; *T* is penetration time, min.

Statistical analysis

Prediction model using multiple linear regression (MLR) analysis

A typical multiple-variable linear regression model is expressed as formula (10):

$$y = k + k_1 \cdot x_1 + k_2 \cdot x_2 + \ldots + k_n \cdot x_n, \quad (10)$$

where: *y* is dependent variable is soil infiltration rate, $mm \cdot min^{-1}$; x_1, x_2, …, x_n are independent variables are bulk density ($g \cdot cm^{-3}$), soil porosity (%), soil moisture (%), organic matter (%), clay (%), silt (%), and sand (%); k, k_1, k_2, …, k_n are regression coefficients.

Using all these parameters basic infiltration rate prediction model was developed using package Bayesian Model Averaging (BMA) in R (programming language).

Bayesian model averaging

Bayesian model averaging (BMA) is a statistical scheme to infer a probabilistic prediction that possesses more skill and reliability than the original ensemble members produced by several competing models (Duan et al. 2007). BMA has been used primarily in generalized linear regression applications. Recently, Bayesian model averaging has gained popularity in diverse fields such as statistics, management science, medicine and meteorology (Fernandez et al. 2001, Raftery et al. 2005).

The key idea behind BMA is to consider a set of models, each with its own set of parameters, and to assign a prior probability to each model. Given the observed data, the posterior probability of each model can then be computed using Bayes' theorem, which takes into account both the likelihood of the data given the model and the prior probability of the model.

Once the posterior probabilities of each model have been computed, they can be used to compute the weighted average of the predictions from each model. This produces a single prediction that takes into account the uncertainty in model selection. The weights used in the averaging process are proportional to the posterior probabilities of each model, so that models with higher posterior probabilities contribute more to the final prediction.

Bayesian information criterion

In inferential statistics, we compare model selections using *p*-values or adjusted R^2. Besides, in this study, we will take the Bayesian predictive model. Analysis of Bayesian model selections using the Bayesian information criterion (*BIC*). *BIC* is defined to be as in formula (11):

$$BIC = n \cdot \ln(1-R^2) + p \cdot \ln(n), \quad (11)$$

where: n is the number of observations in the model, and p is the number of predictors (not including the intercept) in the model.

When the smaller *BIC* value is (more negative), the better the fit of models selected (Schwarz 1978).

Standard deviation (SD) and coefficient of variation (CV)

SD and CV are types of measures of dispersion. SD is an absolute measure and CV is a relative measure. SD and CV are calculated by formulas (12) and (13):

$$SD = \frac{1}{n}\sqrt{\sum_{i=1}^{n}\left(x_i - x'\right)^2}, \quad (12)$$

$$CV = \frac{SD}{x'} \cdot 100, \quad (13)$$

where: x_i is measured value; x' is mean of measured value; n is number of the measured value.

Results and Discussions

Soil infiltration rate

In the sloping land from medium to high rainfall, water infiltration is important for soiling protection and watering retention (Morbidelli et al. 2018). In this study, it was found that the infiltration rate on vegetation types after shifting cultivation (grassland, shrubland and small regenerating trees) varies from 2.41 to 3.23 mm·min^{-1} with a measured average infiltration rate 2.87 ±0.22 mm·min^{-1} (Table 1). Variations in soil infiltration can be induced by vegetation growth and the intrinsic spatial variability of soils. In this study, all vegetation types were restored from shifting cultivation. These shifting cultivation lands were abandoned gradually due to policy-driven factors. The vegetation restoration process improved soil infiltration capacity (Li and Shao 2006, Wang et al. 2012). The improvement in soil infiltration capacity was mainly caused by the growth of vegetation and the resulting changes in soil structure (Pan et al. 2017, Tian et al. 2017).

Soil properties

The soil properties were determined for vegetation recovered after shifting cultivation in Table 2. These were considered

Table 1. Soil infiltration rate (mean ±SD) after shifting cultivation.

Parameter	Min	Max	Mean	Standard deviation	Coefficient of variation
Infiltration rate, mm·min^{-1}	2.41	3.23	2.87	0.22	0.05

Table 2. Descriptive statistics of measured soil properties.

Parameters	Min	Max	Mean	Standard deviation	Coefficient of variation
Bulk density, g·cm^{-3}	1.28	1.48	1.38	0.06	0.00
Soil porosity, %	39.67	47.20	43.58	2.00	4.01
Organic matter, %	1.45	4.65	3.31	0.84	0.70
Soil moisture, %	14.90	25.50	20.08	3.21	10.29
Clay, %	14.43	39.19	24.55	5.54	30.67
Silt, %	16.87	34.06	25.81	5.47	29.90
Sand, %	27.54	68.70	49.64	8.60	74.04

as the independent variables, which were used to establish the correlations between infiltration rate and soil properties and development of the prediction model.

The correlation between infiltration rate and each soil properties

The results in Table 3 showed that *SP*, *OM*, sand have a positive correlation with infiltration rate, which means increase *SP*, *OM* and sand content in the soil will increase the infiltration rate. Whereas *BD*, *SM*, clay and silt have a negative correlation with infiltration rate, which means increasing *BD*, *SM*, clay and silt content in the soil will decrease the infiltration rate. The infiltration rate was significantly affected by *BD*, *SP*, *OM* and *SM* as *R* has varied from 0.77 to 0.86. Whereas clay, silt and sand have a lesser significant effect on the infiltration rate as *R* is only 0.13–0.22.

Different soil properties are influencing infiltration processes. Several studies have been conducted to assess the impact of shifting cultivation on soil properties and its correlation with infiltration rate. Andriesse and Schelhaas (1987) investigated the changes in soil fertility associated with burning in shifting cultivation. They found that burning can lead to a decrease in organic matter content and nutrient availability in the soil, which can ultimately affect the infiltration rate. Ishizuka et al. (2000) found that abandoned land had lower infiltration rates compared to land that was still under shifting cultivation. In addition to organic matter content and nutrient availability, other soil properties can also influence infiltration rate in shifting cultivation. Nye and Greenland

Table 3. Correlation and regression analysis of infiltration rate with soil properties.

Dependent variable	Independent variables	*R*	*F*	*p*	Coefficients	
					Variable	Constant
IR	*BD*	0.80	60.99	< 0.001	-2.969	6.972
	SP	0.77	50.61	< 0.001	0.086	-0.876
	OM	0.86	93.41	< 0.001	0.228	2.121
	SM	0.81	63.44	< 0.001	-0.056	3.998
	Clay	0.21	1.62	0.21	-0.009	3.083
	Silt	0.13	0.60	0.44	-0.005	3.012
	Sand	0.22	1.75	0.19	0.006	2.589

Note: *IR* is infiltration rate, *BD* is bulk density, *SP* is soil porosity, *OM* is organic matter, *SM* is soil moisture.

(1960) reviewed studies on the impacts of shifting cultivation on soil properties and found that cultivation can deteriorate physical soil properties, such as soil structure and compaction, which in turn affect the infiltration rate. Osuji et al. (2010) reported that soil bulk density, soil porosity, organic matters, soil moisture, soil particle size distribution influence the infiltration. An increase in soil bulk density decreases soil porosity resulting in a decrease in soil infiltration characteristics. Results from previous studies also have demonstrated the inverse correlation (Rashidi et al. 2014, Patle et al. 2019). The porosity is one of the aspects that best explains soil infiltration. Ren et al. (2016) found that an increase in porosity could significantly increase soil infiltration. The increase in soil infiltration value is due to porosity, which is related to taproots and the activity of soil organisms (Fischer et al. 2014, Huang et al. 2017). Organic matter is also important for infiltration because it also provides an environment for moesofauna and macrofauna to grow. The stability of organic matter represents an important contribution to the maintenance of the soil porosity. The soil moisture was negatively correlated with *IR* in our study. Water infiltration into the soil diminishes when the soil moisture increases. This result was consistent with the results of previous studies (Assouline 2013, Fouli et al. 2013, Liu et al. 2019), which have proposed that higher soil moisture may lead to a reduction of *IR*. The increase in the soil particle dimension and porosity enhanced soil infiltration capacity directly. Our study showed that a higher soil particle size directly and clay content indirectly enhanced soil infiltration capacity. This result is consistent with those of several studies that have shown that finer-textured soil has a higher hydraulic conductivity than coarse-textured soil due to its well-developed soil structure and a high degree of macropores (Fischer et al. 2014).

Prediction model using multiple linear regression

The effect of soil properties on soil infiltration rate was mentioned not only in a separate factor but also in overall factors (Table 4 and Fig. 2). For prediction of basic infiltration rate, the analysis was categorized into the 5 best models. In the first model, four independent variables were considered: soil porosity, organic matter, soil moisture and sand. The second model included soil porosity, organic matter and soil moisture as independent variables. The third model incorporated soil porosity, organic matter, soil moisture and silt as independent variables. The fourth model featured bulk density, organic matter, soil moisture and sand as independent variables. Lastly, the fifth model encompassed soil porosity, organic matter, soil moisture and clay as independent variables.

Each row corresponds to a variable and each column corresponds to a model; the corresponding rectangle is red if the variable is in the model and yellow otherwise; blue if the variable is a negative correlation with the dependent variable. The width of the column is proportional to the model's posterior probability.

Development of first model

The infiltration rate was estimated using soil porosity, organic matter, soil moisture and sand. The developed prediction equation for the *IR* is given below: $IR = 1.745 + 0.026\ (SP) + 0.016\ (OM) - 0.026\ (SM) + 0.003\ (\text{Sand})$ with the coefficient of determination $R^2 = 0.856$, $BIC = -55.77$

Table 4. Models selected by BMA for regression analysis of infiltration rate with soil properties.

Factor	Post. prob.	Mean	SD	Model 1	Model 2	Model 3	Model 4	Model 5
Intercept	100.0	2.477	1.037	1.745**	1.807**	2.098***	4.099***	1.875**
BD	24.3	-0.155	0.415	-	-	-	-0.950•	-
SP	63.5	0.017	0.016	0.026*	0.028*	0.024*	-	0.029*
OM	100.0	0.115	0.037	0.016**	0.108**	0.112**	0.010*	0.103**
SM	100.0	-0.026	0.007	-0.026***	-0.026***	-0.027***	-0.024**	-0.025***
Clay	20.5	-0.0005	0.002	-	-	-	-	-0.004
Silt	29.8	-0.0013	0.003	-	-	-0.005	-	-
Sand	43.8	0.0017	0.002	0.003•	-	-	0.005*	-
n variable				4	3	4	4	4
R^2				0.857	0.841	0.853	0.850	0.849
BIC				-55.77	-55.38	-54.63	-53.93	-53.83
Post. Prob.				0.165	0.136	0.093	0.066	0.063

Note: Best 5 models of 25 models were selected (cumulative posterior probability = 0.523); Mean ± Standard Deviation (SD) of independent variable; *BIC* is Bayesian Information Criterion; *BD* is bulk density; *SP* is soil porosity; *OM* is organic matter; *SM* is soil moisture; Post. prob. is Posterior probability. Significance codes: (***) < 0.001, (**) < 0.01, (*) < 0.05, (•) < 0.1, ( ) < 1.

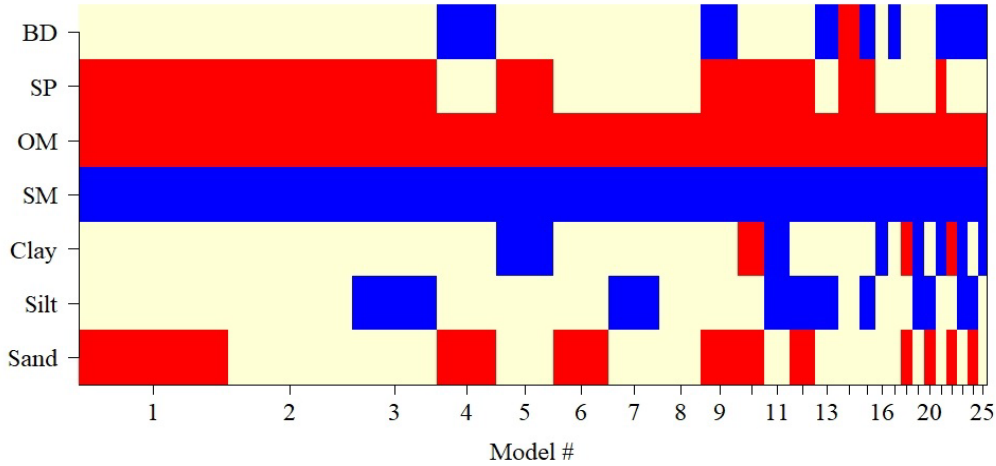

Fig. 2. Models selected by BMA.

and posterior probability = 16.5 %. The *SM* has the lowest *p*-value = 0.0005 (< 0.001), followed by *OM*, *SP* with 0.0018 (< 0.01), 0.0297 (< 0.05), respectively. However, the sand has a *p*-value of 0.0668 (< 0.1). The results showed that *SM*, *OM* and *SP* are statistically significant predictors, while Sand is not an important predictor ($p < 0.05$).

Development of second model

The infiltration rate was estimated using soil porosity, organic matter and

soil moisture. The developed prediction equation for the *IR* is given below: *IR* = 1.807 + 0.028 (*SP*) + 0.108 (*OM*) – 0.026 (*SM*) with the coefficient of determination R^2 = 0.841, *BIC* = – 55.38 and posterior probability = 13.6 %. The *SM* has the lowest *p*-value = 0.0009 (< 0.001), followed by *OM*, *SP* with 0.002 (< 0.01), 0.0244 (< 0.05), respectively. The results showed that *SM*, *OM* and *SP* are statistically significant predictors ($p < 0.05$).

Development of third model

The infiltration rate was estimated using soil porosity, organic matter, soil moisture and silt. The developed prediction equation for the *IR* is given below: *IR* = 2.098 + 0.024 (*SP*) + 0.112 (*OM*) – 0.027 (*SM*) – 0.005 (Silt) with the coefficient of determination R^2 = 0.853, *BIC* = – 54.63 and posterior probability = 9.3 %. The *SM* has the lowest *p*-value = 0.0005 (< 0.001), followed by *OM*, *SP* with 0.0013 (< 0.01), 0.0483 (< 0.05), respectively. However, Silt has a *p*-value of 0.1216 (< 1). The results showed that *SM*, *OM* and *SP* are statistically significant predictors, while silt is not an important predictor ($p < 0.05$).

Development of fourth model

The infiltration rate was estimated using bulk density, organic matter, soil moisture and sand. The developed prediction equation for the *IR* is given below: *IR* = 4.099 – 0.950 (*BD*) + 0.010 (*OM*) – 0.024 (*SM*) + 0.005 (Sand) with coefficient of determination R^2 = 0.85, *BIC* = – 53.93 and posterior probability = 6.6 %. The *SM* has the lowest *p*-value = 0.0022 (< 0.01), followed by *OM*, sand with 0.010 (< 0.05), 0.0164 (< 0.05), respectively. However, the *BD* has a *p*-value of 0.0749 (< 0.1). The results showed that *SM*, *OM* and sand are statistically significant predictors, while BD is not an important predictor ($p < 0.05$).

Development of fifth model

The infiltration rate was estimated using soil porosity, organic matter, soil moisture and clay. The developed prediction equation for the *IR* is given below: *IR* = 1.875 + 0.029 (*SP*) + 0.103 (*OM*) – 0.025 (*SM*) – 0.004 (Clay) with coefficient of determination R^2 = 0.849, *BIC* = – 53.83 and posterior probability = 6.3 %. The *SM* has the lowest *p*-value = 0.0009 (< 0.001), followed by *OM*, *SP* with 0.0031 (< 0.01), 0.0193 (< 0.05), respectively. However, clay has a *p*-value of 0.1894 (< 1). The results showed that *SM*, *OM* and *SP* are statistically significant predictors, while clay is not an important predictor ($p < 0.05$).

For the development of predictive models, from all the analysis, it was observed that the increase in the number of the independent variables increases the reliability of the prediction of R^2. The findings of the present investigation correlate with previous studies. Harisuseno and Cahya (2020) estimated the soil infiltration rate based on soil properties using multiple linear regression. They developed a correlation between soil infiltration rate and soil properties (soil porosity, silt, clay, sand content) with R^2 (0.87). Rashidi et al. (2014) carried out field experiments at the agricultural fields of Karaj (Iran) and developed a correlation between soil infiltration rate and physical properties of soil. They predicted the infiltration rate using silt content and clay content, bulk density, organic matter and moisture content of soil with R^2 (0.9). Pandey and Pandey (2018) conducted a study near the NERIST campus, India, estimating the infiltration rate based on readily available

soil properties (RASPs) in fallow cultivated land. It was found that to predict the soil infiltration rate based on RASPs with seven independent variables (sand, silt, clay, bulk density, particle density, moisture content and organic carbon content) with coefficient of determination R^2 (0.92). Patle et al. (2018) estimated the infiltration rate from soil properties using regression model for cultivated land in India. They predicted the infiltration rate using sand, silt, clay, bulk density, particle density, moisture content and organic carbon content with R^2 (0.80).

The prediction first model had the highest value of posterior probability and lowest value of *BIC*. This implies that the first model is the best amongst all of the models. The use of infiltration models as an alternative to field-based infiltration measurement (Mirzaee et al. 2014, Parhi 2014, Tuffour and Bonsu 2015). Infiltration rate can successfully be measured using a double-ring infiltrometer. However, field-measured infiltration is difficult, especially in mountainous sites. As an alternative, estimating the infiltration rate from soil properties using the regression model. The previous studies reported that easily measurable soil characteristics could successfully predict the measurement of infiltration in the field (Dabral and Pandey 2016, Rahmati 2017).

Conclusion

In this study, the soil porosity, organic matter content and sand have a positive correlation with infiltration rate, whereas bulk density, soil moisture, clay and silt have a negative correlation with infiltration rate. Soil porosity, organic matter and soil moisture were the main factors influencing soil water infiltration capacity. The predicted model with four soil properties (soil porosity, organic matter, soil moisture and sand) was the best-fitted model with the highest value of R^2 and posterior probability and the lowest value of Bayesian information criterion and recommended for the research area. The predictive infiltration model from readily observed soil properties, save the resources in the measurement of time-consuming infiltration characteristics and could be applied under limited data conditions.

References

Andriesse J.P., Schelhaas R.M. 1987. A monitoring study of nutrient cycles in soils used for shifting cultivation under various climatic conditions in tropical Asia. III. The effects of land clearing through burning on fertility level. Agriculture, Ecosystems and Environment 19(4): 311–332. https://doi.org/10.1016/0167-8809(87)90059-4

Assouline S. 2013. Infiltration into soils: conceptual approaches and solutions. Water Resources Research 49(4): 1755–1772. https://doi.org/10.1002/wrcr.20155

Dabral P.P., Pandey P.K. 2016. Models to estimate soil moisture retention limits and saturated hydraulic conductivity. Journal of Indian Water Resources Society 36(1): 50–55. https://iwrs.org.in/journal/jan2016/6jan.pdf

Dionizio E.A., Costa M.H. 2019. Influence of land use and land cover on hydraulic and physical soil properties at the Cerrado Agricultural Frontier. Agriculture 9(24): 9–24. https://doi.org/10.3390/agriculture9010024

Duan Q., Ajami N.K., Gao X., Sorooshian S. 2007. Multi-model ensemble hydrologic prediction using Bayesian model averaging. Advances in Water Resources 30(5): 1371–1386. doi: 10.1016/j.advwatres.2006.11.014

Farid H.U., Mahmood-Khan Z., Ahmad I., Shakoor A., Anjum M.N., Iqbal M.M. 2019. Estimation of infiltration models pa-

rameters and their comparison to simulate the onsite soil infiltration characteristics. International Journal of Agricultural and Biological Engineering 12(3): 84–91. doi: 10.25165/j.ijabe.20191203.4015

Fernandez C., Ley E., Steel M. 2001. Benchmark Priors for Bayesian model averaging. Journal of Econometrics 100(2): 381–427. https://doi.org/10.1016/S0304-4076(00)00076-2

Fischer C., Roscher C., Jensen B., Eisenhauer N., Baade J., Attinger S., Scheu S., Weisser W.W., Schumacher J., Hildebrandt A. 2014. How do earthworms, soil texture and plant composition affect infiltration along an experimental plant diversity gradient in grassland? PloS One 9(2), e98987. https://doi.org/10.1371/journal.pone.0098987

Fouli Y., Cade-Menun B.J., Cutforth H.W. 2013. Freeze-thaw cycles and soil water content effects on infiltration rate of three Saskatchewan soils. Canadian Journal of Soil Science 93(4): 485–496. https://doi.org/10.4141/cjss2012-060

Gee G.W., Bauder J.W. 1986. Particle size analysis. In: Klute A. (Ed.), Methods of soil analysis: physical and mineralogical methods. Part 1. second ed. Soil Science Society of America Inc., Madison, WI: 383–409.

Harisuseno D., Cahya E.N. 2020. Determination of soil infiltration rate equation based on soil properties using multiple linear regression. Journal of Water and Land Development 47(X–XII): 77–88. https://doi.org/10.24425/jwld.2020.135034

Huang Z., Tian F.P., Wu G.L., Liu Y., Dang Z.Q. 2017. Legume grasslands promote precipitation infiltration better than gramineous grasslands in arid regions. Land Degradation Development 28(1): 309–316. https://doi.org/10.1002/ldr.2635

Ishizuka S., Sakurai K., Sabang J., Kendawang I.I., Lee H.S. 2000. Soil characteristics of an abandoned shifting cultivation land in Sarawak, Malaysia. Tropics 10(2): 251–263. doi: 10.3759/tropics.10.251

Karahan G., Yalim Y.Ş. 2022. Evaluation of the relationship between infiltration rate and some soil properties under different land-use. Yuzuncu Yil University Journal of Agricultural Sciences 32(3): 623–634. https://doi.org/10.29133/yyutbd.1130123

Khatri K.L., Smith R.J. 2005. Evaluation of methods for determining infiltration parameters from irrigation advance data. Irrigation and Drainage 54(4): 467–482. https://doi.org/10.1002/ird.198

Li J., He B., Mei X., Liang Y., Xiong J. 2013. Effects of different planting modes on the soil permeability of sloping farmlands in purple soil area. Chinese Journal of Applied Ecology 24(3): 725–731. http://www.cjae.net/EN/Y2013/V24/I3/725

Li Y.Y., Shao M.A. 2006. Change of soil physical properties under longterm natural vegetation restoration in the Loess Plateau of China. Journal of Arid Environments 64(1): 77–96. https://doi.org/10.1016/j.jaridenv.2005.04.005

Liu Y., Cui Z., Huang Z., López-Vicente M., Wu G.L. 2019. Influence of soil moisture and plant roots on the soil infiltration capacity at different stages in arid grasslands of China. Catena 182: 104–147. https://doi.org/10.1016/j.catena.2019.104147

Mirzaee S., Zolfaghari A.A., Gorji M., Dyck M., Ghorbani-Dashtaki S. 2014. Evaluation of infiltration models with different numbers of fitting parameters in different soil texture classes. Archives of Agronomy and Soil Science 60(5): 681–693. https://doi.org/10.1080/03650340.2013.823477

Moazeni-Noghondar S., Golkarian A., Azari M., Asgari Lajayer B. 2021. Study on soil water retention and infiltration rate: a case study in eastern Iran. Environmental Earth Sciences 80(14): 1–18. https://doi.org/10.1007/s12665-021-09760-x

Morbidelli R., Saltalippi C., Flammini A., Govindaraju R.S. 2018. Role of slope on infiltration: A review. Journal of Hydrology 557: 878–886. https://doi.org/10.1016/j.jhydrol.2018.01.019

Neris J., Jimenez C., Fuentes J., Morillas G., Tejedor M. 2012. Vegetation and land–use effects on soil properties and water infiltration of Andisols in Tenerife (Canary Islands, Spain). Catena 98(6): 55–62. https://doi.org/10.1016/j.catena.2012.06.006

Nye P.H., Greenland D.J. 1960. The soil under shifting cultivation. Technical Communication No. 51. Commonwealth Bureau of Soils. Harpenden, Commonwealth Agricultural Bureaux, England, 156 p.

Osuji G.E., Okon M.A., Chukwuma M.C., Nwarie I.I. 2010. Infiltration characteristics of soils under selected land use practises in Owerri, Southeastern Nigeria. World Journal of Agricultural Sciences 6(3): 322–326. https://www.idosi.org/wjas/wjas6(3)/15.pdf

Pan T., Hou S., Wu S., Liu Y., Liu Y., Zou X., Herzberger A., Liu J. 2017. Variation of soil hydraulic properties with alpine grassland degradation in the eastern Tibetan Plateau. Hydrology and Earth System Sciences 21(4): 2249–2261. https://doi.org/10.5194/hess-21-2249-2017

Pandey P.K., Pandey V. 2018. Estimation of infiltration rate from readily available soil properties (RASPs) in fallow cultivated land. Sustainable Water Resources Management 5(2): 921–934. https://doi.org/10.1007/s40899-018-0268-y

Parhi P.K. 2014. Another look at Kostiakov, modified Kostiakov and revised modified Kostiakov infiltration models in water resources applications. International Journal of Agricultural Sciences 4(3): 138–142. https://www.internationalscholarsjournals.com/articles/another-look-at-kostiakov-modified-kostiakov-and-revised-modified-kostiakov-infiltration-models-in-water-resources-appli.pdf

Patle G.T., Sikar T.T., Rawat K.S., Singh S.K. 2018. Estimation of infiltration rate from soil properties using regression model for cultivated land. Geology, Ecology, and Landscapes 3(1): 1–13. https://doi.org/10.1080/24749508.2018.1481633

Raftery A.E., Gneiting T., Balabdaoui F., Polakowski M. 2005. Using bayesian model averaging to calibrate forecast ensembles. Monthly Weather Review 113(5): 1155–1174. https://doi.org/10.1175/MWR2906.1

Rahmati M. 2017. Reliable and accurate point-based prediction of cumulative infiltration using soil readily available characteristics: a comparison between GMDH, ANN, and MLR. Journal of Hydrology 551: 81–91. https://doi.org/10.1016/j.jhydrol.2017.05.046

Rashidi M., Ahmadbeyki A., Hajiaghaei A. 2014. Prediction of soil infiltration rate based on some physical properties of soil. American-Eurasian Journal of Agricultural and Environmental Science 14(12): 1359–1367. doi: 10.5829/idosi.aejaes.2014.14.12.12461

Ren Z., Zhu L., Wang B., Cheng S. 2016. Soil hydraulic conductivity as affected by vegetation restoration age on the Loess Plateau, China. Journal of Arid Land 8(4): 546–555. https://doi.org/10.1007/s40333-016-0010-2

Reynolds B., Reddy K.J. 2012. Infiltration rates in reclaimed surface coal mines. Water Air and Soil Pollution 223(9): 5941–5958. https://doi.org/10.1007/s11270-012-1330-2

Sajjadi S.A.H., Mirzaei M., Nasab A.F., Ghezelje A., Tadayonfar G., Sarkardeh H. 2016. Effect of soil physical properties on infiltration rate. Geomechanics and Engineering 10(6): 727–736. https://doi.org/10.12989/GAE.2016.10.6.727

Saputra D.D., Sari R.R., Hairiah K., Widianto, Suprayogo D., Noordwijk, van Noordwijk M. 2022. Recovery after volcanic ash deposition: vegetation effects on soil organic carbon, soil structure and infiltration rates. Plant and Soil 474: 163–179. https://doi.org/10.1007/s11104-022-05322-7

Schröder L.S., Rasche L., Jantke K., Mishra G., Lange S., Schneider U.A. 2023. Future soil erosion of shifting cultivation on hillslopes – modeling interactions between slope steepness, fallow periods, and climate change, EGU General Assembly, Vienna, Austria, 24–28 Apr 2023, EGU23-13380. https://doi.org/10.5194/egusphere-egu23-13380

Schwarz G. 1978. Estimating the dimension of a model. The Annals of Statistics 6(2): 461–464. http://www.jstor.org/stable/2958889

Sun D., Yang H., Guan D., Yang M., Wu J., Yuan F., Jin C., Wang A., Zhang Y. 2018. The effects of land use change on soil in-

filtration capacity in China: A meta-analysis. Science of the Total Environment 626: 1394–1401. doi: 10.1016/j.scitotenv.2018.01.104

Tang B., Jiao J., Yan F., Li H. 2018. Variations in soil infiltration capacity after vegetation restoration in the hilly and gully regions of the Loess Plateau, China. Journal of Soils and Sediments 19: 1456–1466. https://doi.org/10.1007/s11368-018-2121-1

Tian J., Zhang B., He C., Yang L. 2017. Variability in soil hydraulic conductivity and soil hydrological response under different land covers in the mountainous area of the Heihe River Watershed, Northwest China. Land Degradation and Development 28(4): 1437–1449. https://doi.org/10.1002/ldr.2665

Tuffour H.O., Bonsu M. 2015. Application of Green–Ampt equation to infiltration with soil particle phase. International Journal of Scientific Research in Agricultural Sciences 2(4): 076–088. http://dx.doi.org/10.12983/ijsras-2015-p0076-0088

Wang L., Mu Y., Zhang Q., Jia Z. 2012. Effects of vegetation restoration on soil physical properties in the wind-water erosion region of the Northern Loess Plateau of China. Clean – Soil Air Water 40(1): 7–15. https://doi.org/10.1002/clen.201100367

Wu G.L., Yang Z., Cui Z., Liu Y., Fang N.F., Shi Z.H. 2016. Mixed artificial grasslands with more roots improved mine soil infiltration capacity. Journal of Hydrology 535: 54–60. https://doi.org/10.1016/j.jhydrol.2016.01.059

Zhao Y.G., Wu P.T., Zhao S.W., Feng H. 2013. Variation of soil infiltrability across a 79-year chronosequence of naturally restored grassland on the Loess Plateau, China. Journal of Hydrology 504: 94–103. https://doi.org/10.1016/j.jhydrol.2013.09.039

Zhu P., Zhang G., Wang H., Xing S. 2020. Soil infiltration properties affected by typical plant communities on steep gully slopes on the Loess Plateau of China. Journal of Hydrology 590, 125535. https://doi.org/10.1016/j.jhydrol.2020.125535